

# Finite Temperature Properties of Clusters by Replica Exchange Metadynamics: The Water Nonamer

Yingteng Zhai,<sup>†,‡</sup> Alessandro Laio,<sup>‡,||</sup> Erio Tosatti,<sup>‡,§,||</sup> and Xin-Gao Gong<sup>\*,†</sup>

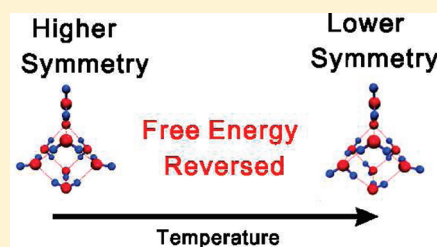
<sup>†</sup>Key Laboratory for Computational Physical Sciences(MOE) and Surface Physics Laboratory & Department of Physics, Fudan University, Shanghai 200433, China

<sup>‡</sup>International School for Advanced Studies (SISSA), via Bonomea 265, 34136 Trieste, Italy

<sup>§</sup>CNR-IOM Democritos National Simulation Centre, via Bonomea 265, 34136 Trieste, Italy

<sup>||</sup>Abdus Salam International Centre for Theoretical Physics (ICTP), Strada Costiera 11, 34014 Trieste, Italy

**ABSTRACT:** We introduce an approach for the accurate calculation of thermal properties of classical nanoclusters. On the basis of a recently developed enhanced sampling technique, replica exchange metadynamics, the method yields the true free energy of each relevant cluster structure, directly sampling its basin and measuring its occupancy in full equilibrium. All entropy sources, whether vibrational, rotational anharmonic, or especially configurational, the latter often forgotten in many cluster studies, are automatically included. For the present demonstration, we choose the water nonamer ( $\text{H}_2\text{O}$ )<sub>9</sub>, an extremely simple cluster, which nonetheless displays a sufficient complexity and interesting physics in its relevant structure spectrum. Within a standard TIP4P potential description of water, we find that the nonamer second relevant structure possesses a higher configurational entropy than the first, so that the two free energies surprisingly cross for increasing temperature.



## INTRODUCTION

The physics of clusters formed by a small number of atoms or molecules is basic to many branches of science.<sup>1</sup> Clusters are the primary nanosystem where matter behaves differently from its usual bulk aggregation. In condensed matter physics, it has long been of interest how collective features of macroscopic systems, such as ordering phenomena and phase transitions, emerge in a nutshell in small size clusters.<sup>2,3</sup> As is well-known, it often proves harder to predict the properties of a small aggregate than those of an infinitely large system, where one can take advantage of regularity. In computational physics, identifying and characterizing cluster structures provide a prototypically difficult optimization problem.<sup>4</sup> The potential energy landscape as a function of the atomic or molecular coordinates is generally complex, with many local minima separated by large barriers even in relatively small clusters, where the simple identification of the lowest energy structure may be a serious computational challenge. State-of-the-art optimization techniques are, for example, sometimes benchmarked on their capability to find the global energy minimum of Lennard-Jones clusters.<sup>5–7</sup> Simulation studies have been devised, using enhanced sampling methods, for example aggregation-volume-bias Monte Carlo and umbrella sampling, to obtain the free energy and density of state of clusters or crystalline nuclei in liquids.<sup>8–11</sup> The recent boost of nanoscience increasingly demands a better ability to characterize, calculate, and understand theoretically the peculiar properties of matter at the nanoscale, a subject of broad technological, practical, as well as conceptual implications.

The traditional manner to approach cluster simulation is quite simple. As a first step, one attempts to identify all the locally stable low energy structures, usually by some global optimization

technique, such as simulated annealing, genetic algorithms, etc. The computational cost of these techniques is largely dominated by repeated potential energy evaluation, and one must carefully choose a level of description of the mechanics of atomic coordinates (quantum or semiempirical or classical) and of the electronic degrees of freedom, allowing at the same time an exhaustive search and a sufficiently accurate estimate of the energy. Sometimes a preliminary search with a less accurate empirical intermolecular potential can be followed by a subsequent refinement leading to a more accurate energy estimate and thus to the identification of the relevant structures with a higher level description. If one is interested in the properties of the system at a very low temperature, what matters is the global energy minimum. When however temperature grows so that  $k_{\text{B}}T$  is comparable to the energy gap  $\Delta_{01}$  above the global minimum, higher energy states become relevant and must be identified. It is traditional to consider a relatively small number of “relevant states”, analogous to inherent states in glass physics, crudely consisting of locally stable atomic configurations or cluster geometries, that identify local energy minima in the space of atomic coordinates. A finite set of relevant states can be obtained, for example, by (real or conceptual) annealing of the system from a much larger number and variety of finite temperature instantaneous molecular configurations, cooled to reach the closest local energy minimum at  $T = 0$ . At finite temperature, each relevant state  $s$  represents the center of a basin in configuration space. The logarithm of the volume of the relevant state basin volume in configuration space represents its entropy  $S_s$ . When the thermal occupancy of each relevant structure  $s$  is

**Received:** August 23, 2010

**Published:** February 3, 2011

explicitly calculable, this is equivalent to specifying its free energy  $F_s = E_s - TS_s$ . A crucial question that needs to be addressed is, what contributes to the entropy of the relevant state, and how it can be properly calculated. The simplest and commonest approach is to consider free rotations and harmonic vibrations around the  $T = 0$  local energy minimum of the relevant state, and calculate the vibrational and rotational entropy involved, in the rigid-rotor-harmonic approximations.<sup>8,12,13</sup> This is, however, not generally adequate, and in fact the rot–vibrational approximation may yield free energies of relevant structures in serious error. For the full entropy of a state, measuring the size of its stability basin should include not just vibrations and rotations, but all possible coordinate transformations leading to essentially equivalent configurations. Proper determination of configurational entropy is a factor that critically reflects the abundance of a relevant state in the cluster's thermal equilibrium. Although these concepts are natural, and well rooted in classic cluster literature,<sup>2,3</sup> they are not always properly implemented in everyday practice where configurational entropy, difficult to define and evaluate, is often overlooked. A practical and accurate calculation approach including automatically all sources of entropy, especially for the more complex molecular clusters, is highly desirable.

In this Article, we introduce and demonstrate a procedure leading to a computationally convenient and conceptually correct extraction of the free energy of the relevant states of a cluster at finite temperature, including all nonelectronic entropy sources contributions. In the simple case we use for our demonstration, a small water cluster, the entropy is found to differ drastically between one relevant state and another. This working case also shows explicitly that the neglect of configurational contributions leads to large errors, totally unacceptable practically no less than conceptually. Our method simultaneously addresses both steps normally followed in traditional cluster study techniques: (a) the search for the relevant structures, and (b) the study of their finite-temperature properties. The approach, based on a recently developed enhanced sampling technique, replica exchange metadynamics,<sup>14</sup> allows the computation of the true free energy of each relevant structure, directly sampling its basin and measuring its occupancy (overall abundance) in full thermal equilibrium, thus including automatically all entropy sources.

For our demonstration purposes, we chose the water nonamer ( $\text{H}_2\text{O}$ )<sub>9</sub>, a very simple dielectric cluster, which nonetheless displays a sufficient complexity and interesting physics in its relevant structure spectrum. Although not directly addressed in this study, well-characterized spectroscopic properties of this particular cluster are available.<sup>15</sup> We studied the cluster properties covering a temperature range of potential interest for atmospheric science (100–250 K) and described the forces between water molecules with a simple but realistic and widely tested empirical force scheme, the so-called TIP4P potential.<sup>16</sup> Because the electronic shells of this system are closed and widely gapped, the use of such effective interatomic forces is not unreasonable, although clearly not definitive. The cluster thermal evolution is simulated by replica exchange metadynamics (RE-META),<sup>14</sup> an approach that requires the simultaneous running of several molecular dynamics simulations at different temperatures. Each simulation (“replica”) is biased by an additional history-dependent “metadynamics potential”.<sup>17</sup> This artificial bias energy term acts on an appropriately chosen small set of collective variables (CV), global or local order parameter-like quantities representing some physically motivated function of molecular coordinates. At fixed time intervals, the replicas are forced to attempt an exchange of their coordinate

configurations. The exchange move is accepted or rejected according to the usual Metropolis criterion,<sup>18,19</sup> including the change of the history dependent CV-based bias potential between the two replicas. The configurations visited in the RE-META simulation correspond to visiting the free energy landscape of the cluster, as a function of the CV variables, in parallel at all temperatures. Combining replica exchange and metadynamics leads to an overall kinetics, which, even at low temperatures, rapidly becomes diffusive in collective variable space, resulting in an extremely efficient configuration sampling.<sup>14</sup> In RE-META, replica exchange is improved because metadynamics explores high free energy configurations within each replica, ultimately leading to faster decorrelation. Metadynamics is in turn strengthened, because replica exchange improves the sampling of the degrees of freedom that are not explicitly biased, thus mitigating one major problem of metadynamics.<sup>14</sup> The water nonamer example confirms that the free energies of the lowest relevant states are indeed heavily affected by configurational entropies. In particular, the entropy of the first excited state is higher than that of the ground state, which causes for increasing temperature an outright crossing of the two free energies and populations, a crossing that does not occur in the vibrational and rotational approximation.

## ■ THE ( $\text{H}_2\text{O}$ )<sub>9</sub> CLUSTER: RE-META CALCULATIONS

For the water nonamer ( $\text{H}_2\text{O}$ )<sub>9</sub>, we carried out RE-META simulations with 11 replicas at the following temperatures: 25.8, 35.8, 47.8, 62.9, 82.4, 108.3, 136.4, 170.0, 205.5, 248.7, and 298.4 K. Because TIP4P bulk ice has a melting temperature of 232 K at 1 bar,<sup>20</sup> the higher temperatures correspond to a fast diffusing liquid-like regime, and the lower ones to a slow diffusing solid-like one. Our level of description is entirely classical, and no quantum effects are included, either nuclear or electronic. Because therefore our treatment ignores all quantum freezing and zero point motion effects, the simulation results lose their strict validity at very low and zero temperatures, a limit where they should not be extrapolated. The molecular dynamics simulation was performed in the NVT ensemble and a cell volume of 18 850 Å<sup>3</sup>, a volume where the probability of observing an isolated water vapor molecule is extremely small. A Nöse–Hoover chain thermostat was used to control the temperature, the integration time step was set to 0.2 fs, and configurations were stored for analysis every picosecond. Each replica was evolved for a total simulation time of 50 ns and independently biased by a metadynamics potential acting on a single collective variable  $S$  counting approximately the number of hydrogen bonds inside the cluster:

$$S(r) = \sum_{ij} \frac{1 - (r_{ij}/r_0)^8}{1 - (r_{ij}/r_0)^{14}} \quad (1)$$

where the sum runs over proton–oxygen pair bonds belonging to different molecules and  $r_0 = 2$  Å. The metadynamics potential has the form:<sup>17</sup>

$$V_G(S(r), t) = w \sum_{\substack{t' = \tau_G, 2\tau_G, \dots \\ t' < t}} \exp\left(-\frac{(S(r) - s(t'))^2}{2\delta_s^2}\right) \quad (2)$$

where  $s(t) = S(r(t))$ ,  $\delta_s = 0.15$ , and  $w = 0.004$  meV. As customary in metadynamics, the collective variable defined in eq 1 is chosen on purely physical grounds and is neither unique nor systematically

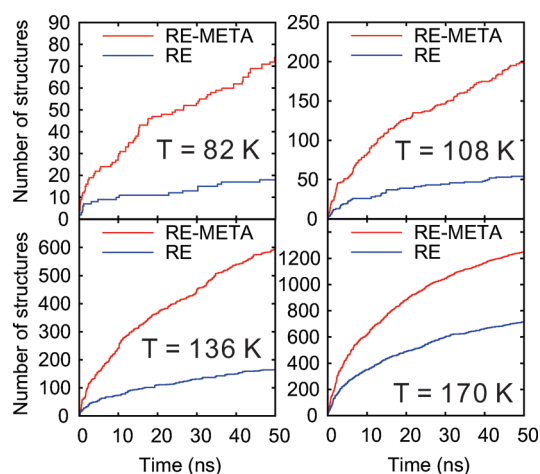


**Figure 1.** The number of relevant states found as a function of simulation time at different temperatures with simple replica exchange (RE) and with RE-META. Note the great improvement brought by addition of the history-dependent metadynamics potential (eq 2), especially important at low temperature.

definable in a general case. However, while this arbitrariness could be seen as endangering the reliability of metadynamics, the replica exchange strategy does, as shown in ref 14, effectively cure the problem. In our calculation, the exchange moves between configurations taken at different temperatures were attempted every 2 ps, accepting the moves with a probability  $\min(1, \exp(-\Delta))$  with

$$\Delta = \beta_i V_i(r_j) + \beta_j V_j(r_i) - \beta_i V_i(r_i) - \beta_j V_j(r_j) \quad (3)$$

where  $i, j$  is the index of the replica,  $V$  is the sum of the potential energy and the bias,  $r$  are the coordinates, and  $\beta$  is the inverse temperature, which is different in each replica.<sup>14</sup> We found that after a typical equilibration time  $\tau_F \approx 4$  ns the history-dependent potential started growing evenly in CV space, meaning independent of  $S$ , in all replicas, indicating that  $-V_G(S, t)$  will eventually, for large  $t$ , provide a good estimate of the free energy as a function of  $S$ .<sup>21</sup> After the equilibration time  $\tau_F$ , we could therefore stop changing the history-dependent potential  $V_G$  and start collecting the statistics of occurrence of properly defined relevant states, with the scope of computing their respective probability, and from that their free energies and entropies in thermal equilibrium.

To analyze the results of the procedure, it is necessary to assign during the MD simulation each molecular coordinate configuration, to the closest reference structure, its relevant state. If all the possible local minima of the potential energy surface were known, one could classify the configurations according to their distance from the reference structures, measured, for instance, by the appropriate root-mean-square deviation of coordinates. This, however, would require a preliminary search of all the minima. More importantly, to assign a configuration to the correct relevant state, one should consider all permutations between identical atoms, a procedure hugely cumbersome and computationally expensive. We apply here a more conservative procedure that uses ideas from the basin hopping technique.<sup>6</sup> Starting from all the coordinate configurations generated by MD, we carried out a static potential energy minimization by conjugate gradients evolving atomic coordinates until the force on each atom was less than 0.0001 eV/Å. If a reference structure with the same potential energy is already available, the instantaneous MD configuration is

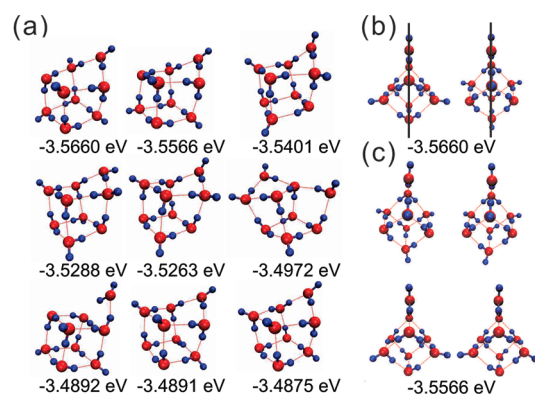


**Figure 2.** (a) Lowest energy relevant states of the water nonamer. (b) Front and back viewed configurations for state 0 (lowest energy state). Black line: Symmetry plane. (c) Front and back viewed configurations for state 1 (second lowest state). For a fixed oxygen skeleton, state 1 has twice larger multiplicity than state 0, which has a mirror symmetry. Thus, the configurational entropy of state 1 may be expected to exceed that of state 0 by approximately  $\ln 2$ .

assigned to that structure. Otherwise, a new reference structure is introduced in the pool. Here, two quenched structures are assumed to be the same if their energy difference is smaller than 0.0001 eV. This procedure is still computationally intensive, but allows an unambiguous assignment of all MD frames and is insensitive to permutation of the atoms.

Figure 1 shows the number of independent structures that are explored as a function of simulation time at different temperatures for a normal replica exchange run, which we carried out in parallel for comparison, and for RE-META. The number of structures visited is much larger in the latter, a beneficial result of the metadynamic bias technique, especially important at low temperature. This demonstrates how RE-META can be successfully used to carry out the first task normally undertaken in cluster studies, the search for all the low energy relevant structures.

Figure 2a shows the molecular structure of the water nonamer lowest energy relevant structures. The five lowest energy structures share the same oxygen arrangement and differ only by the position of the protons. Eight oxygens form a regular hexahedron, and an additional oxygen is attached to one of the edges. The global minimum is identical to that previously identified in ref 22. In all of the nine relevant structures, 13 H-bonds are formed.

As seen in Figure 2, the lowest energy structure has a mirror symmetry about the plane shown as a black line in Figure 2b, while the same mirror plane gives rise to two distinguishable degenerate structures for the second lowest structure. This, as we will see in the following, significantly influences their respective configurational entropies.

We now come to our main point. Besides providing a tool for the quick exploration of cluster structures, RE-META crucially yields an accurate estimate of the probability to observe each relevant structure  $S$  as a function of temperature. Following ref 23, we first compute the average bias potential:

$$V_G(S) = 1/(\tau_{\text{sim}} - \tau_F) \int_{\tau_F}^{\tau_{\text{sim}}} dt V_G(S, t) \quad (4)$$

where  $\tau_F$  is the equilibration time of  $V_G$ , 4 ns in this work, and  $\tau_{\text{sim}}$  is the total simulation time. Denoting by  $r_i$  all the configurations



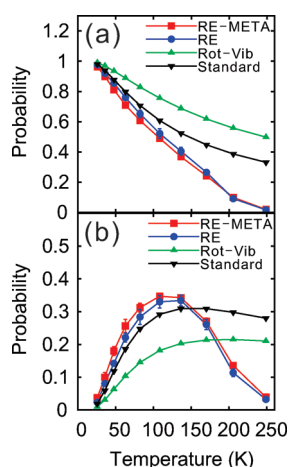


**Figure 3.** (a) Occupancy probability for the lowest energy relevant state (“0”) versus temperature, with RE-META, normal RE, rigid-rotor-harmonic approximation (“rot–vib”), and rigid-rotor-harmonic approximation with an additional  $\ln 2$  factor in the entropy of state 1–state 8 (“standard”). (b) Occupancy probability for the second lowest energy relevant state (“1”). The statistical error bars in RE and RE-META represent the standard deviations estimated by separately comparing averages in three successive portions of the simulations. Note the substantial agreement between RE and RE-META and the large deviation of the rot–vib approximation, showing its clear inadequacy. Note also that the occupancies of states computed with RE and RE-META are fully consistent with those computed using the standard approach at low temperature, and how the probability of state 1 overtakes that of state 0 around 150 K, as a result of its larger configuration entropy.

generated by RE-META at temperature  $T$ , we estimate the equilibrium probability to observe relevant structure  $\alpha$  as

$$p^\alpha(T) = \frac{\sum_{i \in \alpha} \exp(V_G(S(r_i))/k_B T)}{\sum_{\beta} \sum_{i \in \beta} \exp(V_G(S(r_i))/k_B T)} \quad (5)$$

where the notation  $i \in \alpha$  means that the sum runs over the configurations that are assigned to structure  $\alpha$  as explained above. To assess the reliability of this approach, we also computed the probability  $p_\alpha$  in normal replica exchange where the probability is simply proportional to the number of times the structure  $\alpha$  is observed. As shown in Figure 3a,b, the probabilities estimated in the two manners are consistent. The small remaining discrepancy between RE and RE-META is due to statistical uncertainties. We remark that the errors of methods based on statistical sampling are inevitably large at low  $T$ , as the relevant transitions are observed relatively rarely even if a powerful enhanced sampling approach is used.

## ■ COMPARISON BETWEEN RE-META AND RIGID-ROTOR-HARMONIC VIBRATION APPROXIMATIONS

We calculate and compare in Figure 3a,b the exact occupancy probabilities of the two lowest relevant structures with the approximate probabilities, now estimated using the rigid-rotor-harmonic vibration approximation to the cluster vibrational spectrum of each state:

$$p^\alpha(T) = \frac{\exp(-F^\alpha/k_B T)}{\sum_{\beta} \exp(-F^\beta/k_B T)} \quad (6)$$

where the rigid-rotor-harmonic free energies  $F^\alpha$  are calculated

as

$$F^\alpha = E^\alpha - kT \ln q_{\text{rot-vib}}^\alpha \quad (7)$$

where  $E^\alpha$  is the energy and

$$q_{\text{rot-vib}}^\alpha = q_{\text{rot}}^\alpha + q_{\text{vib}}^\alpha \quad (8)$$

$$q_{\text{rot}}^\alpha = \left( \frac{8\pi^3 k_B T}{h^2} \right)^{3/2} \frac{\prod_{i=1}^3 \sqrt{I_i^\alpha}}{\sigma^\alpha \pi} \quad (9)$$

$$q_{\text{vib}}^\alpha = \prod_m \frac{k_B T}{h \omega_m^\alpha} \quad (10)$$

where  $I_i^\alpha$  are the principal moments of inertia,  $\sigma^\alpha$  is the rotational symmetry number, and  $\omega_m^\alpha$  is the vibrational frequency of mode  $m$  obtained by diagonalizing the Hessian matrix of the potential in structure  $\alpha$  at  $T = 0$ . To keep the calculation simple, the summation in the denominator of eq 6 runs over the nine lowest energy states. We have checked that if 30 structures are included in the summation, the probability to observe all states between the 9th and 30th is only 0.2% at 108 K and 13% at the highest temperature 250 K. It should be noticed that the rotational symmetry numbers of the lowest energy relevant states of the water nonamer are all equal to 1 and the moments of inertia are similar. So, for this system, the rotational entropy varies much less than the vibrational entropy. For example, the rotational entropy difference between state 0 and state 1 is only 7% of the vibrational entropy difference. As is seen in Figure 3, the true occupancy probabilities from RE-META and those predicted by the rigid-rotor-harmonic vibration approximation eq 6 differ very significantly. For instance, at  $T = 200$  K, eq 6 still predicts a significant population for state 0 and state 1, while RE-META shows that the population of state 0 has become negligible, while the population of state 1 is only about 10%. Moreover, the rot–vib approximation eq 6 implies that state 0 is always more populated than state 1, whereas according to RE-META the most populated state at 150 K is state 1 and not state 0.

We finally calculated the entropy difference between states 0 and 1:

$$\Delta S = \frac{\Delta E - \Delta F}{k_B T} \quad (11)$$

where  $\Delta F$  and  $\Delta E$  are the free energy and the internal energy differences. Figure 4 shows the entropy difference estimated with RE-META, RE, and rot–vib approximation. This entropy difference is finite and of order 1 even at the lower temperatures signaling an initial configurational degeneracy of state 1, and grows further upon heating. The rot–vib approximation, on the other hand, misses both effects. Visual inspection of the structures assigned to relevant states 0 and 1 (data not shown) reveals that up to  $T = 200$  K the oxygen skeleton remains largely unchanged. Thus, the main source of configurational entropy is proton disorder.

The state 0 has a mirror symmetry, while state 1 does not. The broken symmetry implies that state 1 is 2-fold degenerate. Thus, the relative configurational entropy of state 1 is roughly  $\ln 2$ , which, at low temperature, approximately agrees with the relatively large occupancy of state 1. Adding  $\ln 2$  to the rot–vib entropy for states (but not for state 0) leads to a positive “standard”

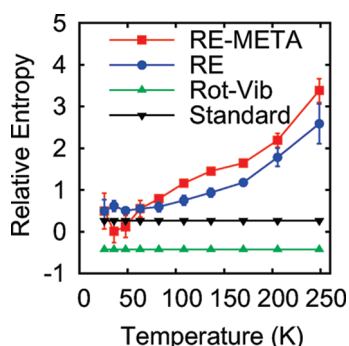


**Figure 4.** Entropy difference between state 1 and state 0 as a function of  $T$ . Note the initially larger configurational entropy of state 1, further growing with temperature, due to anharmonicity. Both effects are missed by the rot–vib approximation, whereas the addition of  $\ln 2$  (the “standard” approximation) provides a reliable result only well below 100 K.

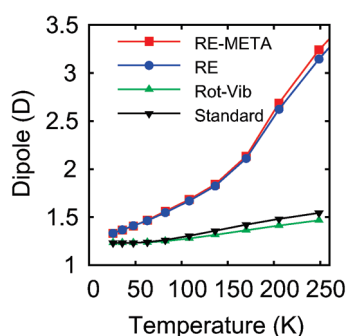


**Figure 5.** Thermal averaged dipole moment of a water nonamer, computed directly from the RE-META and RE trajectories and using the probabilities (eq 6) estimated within the “rot–vib” and “standard” approximation.

entropy difference (black curve in Figure 4), closer to the simulation results at small  $T$ . At high temperature, anharmonic contributions further favor state 1, making the entropy difference estimated even with the standard approach unreliable. Consistently, as shown in Figure 3, the occupancies estimated with the standard approach are compatible with those estimated with RE-META at low  $T$ , but important deviations appear at  $T > 100$  K. The comparison of the occupancies presented in Figure 3 and, even more, of the entropy differences of Figure 4 is the central result of this work.

## DISCUSSION AND CONCLUSIONS

The cluster description obtained with RE-META can naturally be used to predict measurable quantities. As an example, we computed the average dipole of the water nonamer as a function of  $T$ . In Figure 5, the accurate RE-META computed dipole is compared to the rot–vib approximation:  $D = \sum_{\alpha} D^{\alpha} p^{\alpha}(T)$ , where  $D^{\alpha}$  is the dipole in the reference structure  $\alpha$  and the probabilities  $p^{\alpha}$  are estimated by eq 6. The exact and the approximate results differ very significantly, underlining the devastating effects of ignoring the configurational and anharmonic entropies, especially at high  $T$ .

Beyond the deliberately simple case study  $(\text{H}_2\text{O})_9$  presented here, RE-META method is applicable to larger water clusters, and of course to different systems, once the collective variables are properly selected. The workload and complexity grow considerably

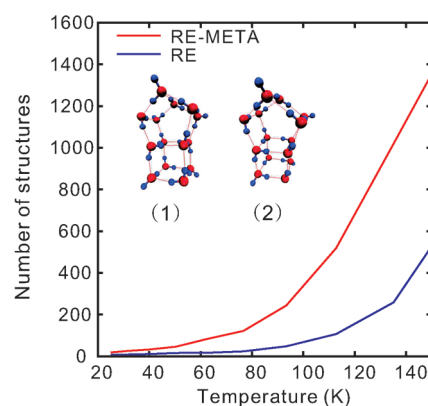


**Figure 6.** The number of relevant states of  $(\text{H}_2\text{O})_{14}$  found as a function of temperature with simple replica exchange and with RE-META. Improvement brought by RE-META method is also notable. Insets: (1) Lowest relevant state; (2) second lowest relevant state.

with size, not surprisingly in view of the exponential growth of phase space, but the effectiveness is not impaired. As an example, we considered the larger water cluster  $(\text{H}_2\text{O})_{14}$ , hundreds of times more complex than the nonamer, with a 10 ns simulation. Figure 6 shows the number of independent structures explored as a function of simulation temperatures for RE and RE-META, underlining the strong superiority of the latter, in particular its ability to unearth relevant structures that would otherwise be simply ignored.

In summary, we have shown how the full configurational complexity of a small cluster can be directly, realistically, and economically accessed by a suitable sampling, combining replica exchange with metadynamics techniques (RE-META). This proves extremely effective in searching the cluster’s relevant states, and in measuring their thermal population as a function of  $T$ . In the water nonamer, these populations are shown to differ largely from those routinely predicted by rot–vib approximation. The crucial factor that influences the populations is the configurational entropy of the relevant states, an entropy that is generally inaccessible but that in RE-META is naturally and directly measured and understood. The method holds a good promise of applicability in a great variety of relevant systems, provided a set of good, physically motivated collective variables can be identified.

## AUTHOR INFORMATION

### Corresponding Author

xggong@fudan.edu.cn

## ACKNOWLEDGMENT

E.T. dedicates his work in this paper to the memory of Victoria Buch. E.T. acknowledges hospitality at Fudan, where this work began. Y.Z. acknowledges hospitality at SISSA, where this work was mainly carried on. Work at Fudan is partially supported by the National Science Foundation of China, by special funds for major state basic research, by the research program of Shanghai municipality, and by MOE. Work in Trieste is supported by the ESF EUROCORE FANAS project AFRI sponsored by CNR and by PRIN-COFIN 20087NX9Y7 contract of the Italian University and Research Ministry.

## REFERENCES

- (1) Baletto, F.; Ferrando, R. *Rev. Mod. Phys.* **2005**, *77*, 371–423.

- (2) Wales, D. J.; Berry, R. S. *Phys. Rev. Lett.* **1994**, *73*, 287–52878.
- (3) Proykova, A.; Berry, R. S. *J. Phys. B: At., Mol. Opt. Phys.* **2006**, *39*, R167–R202.
- (4) Wales, D. J.; Doye, J. P. K.; Miller, M. A.; Mortenson, P. N.; Walsh, T. R. *Adv. Chem. Phys.* **2000**, *115*, 1–111.
- (5) Beck, T. L.; Jellinek, J.; Berry, R. S. *J. Chem. Phys.* **1987**, *87*, 545–554.
- (6) Wales, D. J.; Doye, J. P. K. *J. Phys. Chem. A* **1997**, *101*, 5111–5116.
- (7) Gregor, T.; Car, R. *Chem. Phys. Lett.* **2005**, *412*, 125–130.
- (8) Li, Z. H.; Bhatt, D.; Schultz, N. E.; Siepmann, J. I.; Truhlar, D. G. *J. Phys. Chem. C* **2007**, *111*, 16227–16242.
- (9) Chen, B.; Siepmann, J. I.; Klein, M. L. *J. Phys. Chem. A* **2005**, *109*, 1137–1145.
- (10) Rein ten Wolde, P.; Oxtoby, D. W.; Frenkel, D. *Phys. Rev. Lett.* **1998**, *81*, 3695–3698.
- (11) Li, Z. H.; Truhlar, D. G. *J. Am. Chem. Soc.* **2008**, *130*, 12698–12711.
- (12) Li, Z. H.; Jasper, A. W.; Truhlar, D. G. *J. Am. Chem. Soc.* **2007**, *129*, 14899–14910.
- (13) Adjanor, G.; Athènes, M.; Calvo, F. *Eur. Phys. J. B* **2006**, *53*, 47–60.
- (14) Bussi, G.; Gervasio, F. L.; Laio, A.; Parrinello, M. *J. Am. Chem. Soc.* **2006**, *128*, 13435–13441.
- (15) Andersson, P.; Steinbach, C.; Buck, U. *Eur. Phys. J. D* **2003**, *24*, 53–56.
- (16) Jorgensen, W. L.; Chandrasekhar, J.; Madura, J. D.; Impey, R. W.; Klein, M. L. *J. Chem. Phys.* **1983**, *79*, 926–935.
- (17) Laio, A.; Parrinello, M. *Proc. Natl. Acad. Sci. U.S.A.* **2002**, *99*, 12562–12566.
- (18) Thijssen, J. M. *Computational Physics*, 2nd ed.; Cambridge University Press: New York, 2007.
- (19) Sugita, Y.; Okamoto, Y. *Chem. Phys. Lett.* **1999**, *314*, 141–151.
- (20) Vega, C.; Sanz, E.; Abascal, J. L. F. *J. Chem. Phys.* **2005**, *122*, 114507.
- (21) Laio, A.; Gervasio, F. L. *Rep. Prog. Phys.* **2008**, *71*, 126601.
- (22) Brudermann, J.; Buck, U.; Buch, V. *J. Phys. Chem. A* **2002**, *106*, 453–457.
- (23) Marinelli, F.; Pietrucci, F.; Laio, A.; Piana, S. *PLoS Comput. Biol.* **2009**, *5*, e1000452.